Spin-glass ordering in $Zn_{1-x}Mn_xIn_2Te_4$ diluted magnetic semiconductor

G. F. Goya*
Instituto de Física, Universidade de São Paulo, CP33618, 05315-970 São Paulo, Brazil

V. Sagredo
Departamento de Física, Facultad de Ciencias, Universidad de los Andes, Mérida, Venezuela

(Received 26 February 2001; revised manuscript received 9 September 2001; published 27 November 2001)

We present a study of the magnetic properties of the $Zn_{1-x}Mn_xIn_2Te_4$ diluted magnetic semiconductor for concentrations $0.3 \leqslant x \leqslant 1.0$. Samples with $x \leqslant 0.5$ displayed a paramagnetic behavior down to the lowest experimental temperature (1.8 K), whereas a paramagnetic to spin-glass transition was observed for $x > 0.5$ at temperatures 2.5 K $\leqslant T \leqslant$ 3.8 K, depending on the Mn content. The effective magnetic moment $\mu_{eff} = 5.80(2)\mu_B$, calculated from the high-temperature susceptibility, corresponds to a $3d^5$ ($S = \frac{5}{2}$) configuration for Mn^{2+}. For the sample with composition $x = 0.9$, the in-phase component of the ac susceptibility has been analyzed according to conventional power-law dynamics, obtaining a freezing temperature of $T_f = 3.1(2)$ K and a critical exponent $z\nu = 10.3 \pm 2$. Low-field dc magnetic susceptibility data show a sharp peak at ~ 3.3 K, below which strong irreversibility is observed between zero-field-cooled and field-cooled states. Evidence of a true phase-transition phenomenon is given by the steep increase of the nonlinear susceptibility χ_{nl} when approaching T_f from above. A static scaling of χ_{nl} yielded values $\beta = 0.9(1)$ and $\gamma = 3.6(4)$ for the critical exponents, and gave also the proper asymptotic behavior of the scaling function. These values are in good agreement with data reported for other spin-glasses such as $M_{1-x}Mn_xTe$ (M = Zn, Cd, and Hg), and constitute strong evidence of a three-dimensional spin-glass transition in $Zn_{1-x}Mn_xIn_2Te_4$.

DOI: 10.1103/PhysRevB.64.235208 PACS number(s): 75.50.Lk, 75.50.Pp, 75.25.+z, 75.40.Cx

I. INTRODUCTION

Diluted magnetic semiconductor (DMS) spin systems with structural or compositional random disorder have interesting magnetic properties from both theoretical and experimental points of view. In recent years, considerable efforts have been focused on solving two leading issues: (1) the spin-glass (SG) problem, and (2) the ground state in random magnetic systems with magnetic long-range order.[1–3] Both issues could be studied in a single solid solution at different degrees of magnetic dilution, provided that no structural phase transitions take place at intermediate concentrations, a situation seldom observed in doped DMS systems. Related to the existence of a spin-glass transition, the question of whether it is a true phase transition in the thermodynamic sense or a gradual freezing of the magnetic moments has been discussed for more than two decades.[4] As a consequence, there is a necessity for comparative studies on experimental systems with spin-glass behavior in order to scrutinize critical theories. In this context, we present a detailed characterization of the critical behavior of a semiconducting system, showing typical SG properties.

Regarding the critical parameters that govern the SG transition, Ising and Heisenberg models have been used to calculate the internal energy, exchange constant, and correlation length of spin glasses in the critical region. Although no analytical solutions exist for three-dimensional (3D) models, Monte Carlo simulation and high-temperature series expansions have given solid evidence supporting the existence of a phase transition at finite temperatures.[5,6] Another line of research was traditionally devoted to finding the kind of interactions responsible for the SG state. It is now well established that, irrespective of its dimensionality, the magnetic frustration necessary for a SG state may originate from two main effects: (1) topological properties of the magnetic lattice, as in $Zn_{1-x}Mn_xTe$ (Ref. 7) and $SrCr_8Ga_4O_{19}$,[8] or (2) competing exchange interactions as in canonical spin glasses like CuMn (Ref. 9) and insulating $Eu_xSr_{1-x}S$.[10]

DMS systems of composition II-III_2-VI_4 (where II and III are transition metals and VI = S, Se, Te) crystallize in a variety of structures with different number of octahedral Ω and tetrahedral Γ sites per unit cell. For example, in the spinel structure there are $(2\Omega + \Gamma)$ sites; in laminar structures $(\Omega + 2\Gamma)$ sites, and tetragonal structures have (3Ω) sites. Different models have been proposed to describe the distribution of II and III atoms among Ω and Γ sites in these structures, from random to fully ordered occupation patterns,[11–13] but each compound has too many particularities to extract general rules. However, it is now accepted that the main factors that govern ionic order are cation-anion atomic radii as well as cation affinity for octahedral or tetrahedral coordination.[14]

The MIn_2Te_4 family of compounds adopts a defective chalcopyrite structure when M = Zn or Mn. In this case, the crystal lattice may be described as a set of Te anions occupying the crystal $8(i)$ sites, tetrahedrally coordinated with M and In cations at $4(d)$ and $2(a)$ sites respectively. Range and Hubner[15] proposed a model for $MnIn_2Te_4$, in which both Mn and In ions are randomly distributed over the accessible Ω and Γ sites. The defective nature of the structure is reflected in the pseudotetrahedral coordination of the Te anions, i.e., there is a vacancy at one vertex of the coordination tetrahedron (the $2d$ site). These two features (random distribution of magnetic ions and the ordered arrangement of vacancies, which breaks superexchange Mn-Te-Mn paths) make these compounds very promising for testing critical theories, and

should be included in the description of the magnetically ordered state. Since both $ZnIn_2Te_4$ and $MnIn_2Te_4$ have the same defective chalcopyrite structure (space group $I\bar{4}2m$), the $Zn_{1-x}Mn_xIn_2Te_4$ solid solution is expected to display full solubility for the whole x range, as verified experimentally.[16] The absence of phase transitions between the end members of the solid solution also enables one to investigate whether the characteristic quantities of a spin glass can be scaled to x. With the above notions in mind, we have undertaken a study on the magnetic properties of a $Zn_{1-x}Mn_xIn_2Te_4$ solid solution with $0.3 \leqslant x \leqslant 1.0$, using dc and ac magnetic measurements in both the low-temperature critical region and the paramagnetic (high-temperature) regime.

The organization of the present paper is as follows: In Sec. II, the experimental details are described. In Sec. III the results are presented and discussed in three parts. Section III A deals with an analysis of the paramagnetic, high-temperature data. A dynamical analysis of the ac susceptibility is presented in Sec. III B, and the static scaling of the dc magnetization in Sec. III C. Finally, a discussion and conclusions drawn from the present work are given in Sec. IV.

II. EXPERIMENTS

Samples of $Zn_{1-x}Mn_xIn_2Te_4$ with $0.3 \leqslant x \leqslant 1.0$ for the present work were produced by a fusion-controlled method. The components were sealed under vacuum in small quartz ampoules, previously carbonized to prevent contamination, and melted together at $T = 1000\,^{\circ}C$ for 24 h. Samples were then slowly cooled to room temperature in four days. Atomic absorption technique was used to determine Mn content. Structural data of $Zn_{1-x}Mn_xIn_2Te_4$ as a function of x were previously reported,[16] showing regular increments of a and c cell parameters with increasing Mn^{2+} contents, in agreement with its larger ionic radius compared to Zn^{2+}. At room temperature, x-ray patterns were indexed as a single-phase chalcopyrite-type structure (space group $I\bar{4}2m$), without signs of structural transitions along the series.

To perform magnetic measurements, small crystallites of these samples were dispersed in epoxy resin, and molded in cylindrical shape of diameter 5 mm and height 3 mm. Magnetization measurements were performed in a commercial superconducting quantum interference device magnetometer in both zero-field-cooling (ZFC) and field-cooling (FC) modes, between 1.8 K $\leqslant T \leqslant$ 300 K and applied fields up to 7 Tesla. In all cases, the diamagnetic contribution of the sample holder was subtracted, and the resulting susceptibilities were further corrected for core diamagnetism of the ions. Within the $T \approx T_f$ region, measurements of $M(T)$ and ac susceptibility were performed in small ($\Delta T < 0.1$ K) steps and measuring times ~ 10 min at each point, to determine the transition temperature. In order to study the frequency-dependent cusp of the in-phase $\chi'(T)$ and out-of-phase $\chi''(T)$ components of the ac magnetic susceptibility, data were measured at driving frequencies between 10 mHz $\leqslant f \leqslant 2$ kHz.

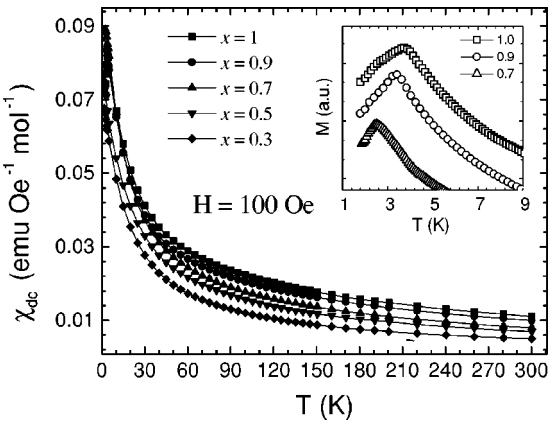

FIG. 1. dc magnetic susceptibility $\chi_{dc}(T) = M/H$ for $Zn_{1-x}Mn_xIn_2Te_4$, taken with $H = 100$ Oe. Inset: Magnification of the low-temperature region for ZFC curves measured (on heating) using $H_{dc} = 10$ Oe, for $x = 1.0$, 0.9, and 0.7. Each curve shows a maximum at $T_M = 3.8(1)$, 3.3(1), and 2.5(2) K, respectively.

III. RESULTS AND DISCUSSION

A. Paramagnetic regime

Figure 1 shows the experimental dc magnetic susceptibility $\chi_{dc}(T) = M(T)/H$ measured in the ZFC mode with $H_{FC} = 100$ Oe, from 1.8 to 300 K, for the whole $Zn_{1-x}Mn_xIn_2Te_4$ series. Samples with $x = 0.3$ and 0.5 displayed paramagnetic behavior down to the lowest experimental temperature. For samples with $x \geqslant 0.7$ a peak in $M(T)$ was found at a temperature labeled T_M, which depends on the Mn concentration (see the inset of Fig. 1, and Table I). The nature of these transitions will be discussed below.

The inverse magnetic susceptibility $\chi_{dc}^{-1}(T)$ follows a linear dependence with T at high temperatures for the whole x range. However, deviations from the $\chi^{-1} \propto T$ regime are noticed for $T \leqslant 100$ K, especially in samples with $x \geqslant 0.5$. We associate this behavior with the onset of superexchange interactions between Mn ions in Mn-rich samples, since for $x = 0.7$ we are clearly above the percolation threshold. To investigate the dependence of both the molar Curie constant (C) and Curie-Weiss temperature (Θ) on x, we used an expression of the static magnetic susceptibility $\chi(T)$ derived for a randomly disordered Heisenberg antiferromagnet. The Hamiltonian representing such a system may be written as[17]

TABLE I. Effective magnetic moment μ_{eff}, Weiss constant Θ, and freezing temperature T_M (observed from dc magnetization data) as a function of x in $Zn_{1-x}Mn_xIn_2Te_4$.

Mn content	T_M (K)	$\mu_{eff}(\mu_B)$	Θ(K)
$x = 1.0$	3.8(1)	5.80(2)	−98(4)
$x = 0.9$	3.3(1)	5.60(2)	−84(4)
$x = 0.7$	2.5(2)	4.79(3)	−63(6)
$x = 0.5$	< 1.8	4.36(4)	−56(6)
$x = 0.3$	< 1.8	3.60(4)	−38(6)

$$H=\sum_{i,j} J_{ij}\mathbf{S}_i\cdot\mathbf{S}_j\xi_i\xi_j-\mathbf{g}\mu_B\mathbf{H}\cdot\sum_i \mathbf{S}_i\xi_i \qquad (1)$$

where **g** is the gyromagnetic factor, μ_B the Bohr magneton, J_{ij} the exchange constant, and the sum runs over all lattice sites. The scalar ξ_i can take values 1 or 0, depending on whether the ith site is occupied by a magnetic or nonmagnetic ion, respectively. Therefore the set $\{\xi_i\}$ determines each possible distribution of magnetic ions with spin $\mathbf{S}_i$ within the lattice. The expression for the susceptibility is then derived from the usual partition function, yielding

$$\chi(T)=g^2\mu_B^2\beta_B\sum_{i,j}\overline{\langle\xi_i\xi_jS_i^zS_j^z\rangle_{T,H=0}}, \qquad (2)$$

where k_B is the Boltzmann constant and $\beta_B=(k_BT)^{-1}$. The $\overline{\langle\cdots\rangle}$ operation represents the configurational average over all equivalent sets $\{\xi_i\}$. For a randomly disordered system, these averages can be easily estimated in the high-temperature limit, for in this case the product $\overline{\xi_i\xi_j}$ satisfies $\overline{\xi_i^2}=x$ for $i=j$ and $\overline{\xi_i\xi_j}=x^2$ for $i\neq j$, where x is the fraction of magnetic ions in the lattice. Expansion of $\chi^{-1}(T)$ to first order in β_B then yields a Curie-Weiss law

$$\chi^{-1}(T,x)=\frac{T-\Theta(x)}{C(x)}, \qquad (3)$$

with

$$C(x)=\frac{S(S+1)g^2\mu_B^2N_A}{3k_B}x=C_0x, \qquad (4)$$

$$\Theta(x)=\frac{-2S(S+1)}{3k_B}x\sum_i J_iz_i=\Theta_0x, \qquad (5)$$

and N_A Avogadro's number. The expression of Θ_0 contains the sum of exchange integrals J_i between a given atom and the number z_i of ith neighbors. In the above derivation, it was also assumed that the orbital moment of Mn^{2+} ions are quenched (i.e., $L=0$), so the spin-only value $S=\frac{5}{2}$ can be used for atomic moments. This assumption is in agreement with previous EPR measurements on these samples,[16] and is also consistent with the values of effective Mn moment obtained from susceptibility data (see below).

The experimental data could be well fitted with Eq. (3) in the high-temperature ($T\geqslant 150$ K) region, as shown in Fig. 2. The resulting values of the Curie-Weiss temperature Θ were negative for the whole x range, indicating predominant antiferromagnetic (AFM) superexchange interactions between Mn ions. The effective moment $\mu_{eff}=5.80(2)\mu_B$ obtained for $x=1.0$ (see Table I) is slightly smaller than the spin-only value for the $3d^5$ atomic configuration of Mn^{2+} ($S=\frac{5}{2}$ state, $\mu_{eff}=5.92\mu_B$). One possible reason for this difference might be the partial covalent character of the p-d (Mn^{2+}-Te^{2-}) bonds. Previous estimations of the p-d admixture for Mn^{2+}-X^{2-} bonds in II-IV semiconductors,[17] using perturbed p^* and d atomic functions $p^*=(1+b^2)^{-1/2}(p+bd)$, where b represents the amount of p-d mixing, yielded a value $\Delta S/S=b^2\simeq 0.04$. A second possibility might be the presence of a small amount ($\simeq 10\%$) of Mn^{3+} ($S=2,\mu_{eff}=4.9\mu_B$), which could also yield the observed low-S value.

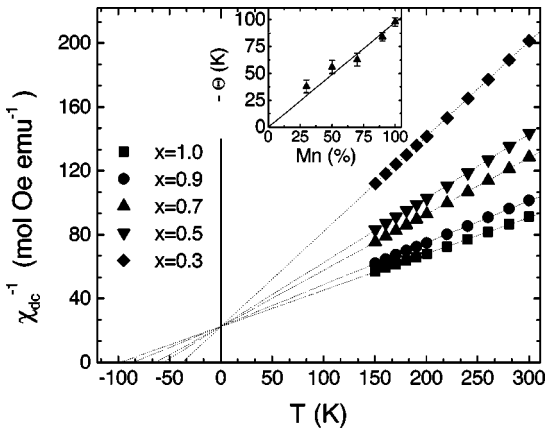

FIG. 2. Inverse of the magnetic susceptibility $\chi^{-1}(T)$ in the paramagnetic regime ($T\geqslant 150$ K). Fits using Eq. (3) are shown by dotted lines. Note that there is a common intercept on the y axis for all concentrations. Inset: The obtained values of $\Theta(x)$ plotted as a function of x. The solid line is the best linear fit, which corresponds to $\Theta_0=-98(4)$ K.

It can be seen from Eqs. (4) and (5) that for a randomly dilute AFM the macroscopic parameters C and Θ must scale linearly with the Mn concentration. The inset of Fig. 2 shows that for $\Theta(x)$ this trend is approximate, and the best linear fit yielded $\Theta_0=-98(4)$ K, coincident with the value of $\Theta(x=1)$ within experimental error. Another consequence of Eq. (3) is that the extrapolation of the $\chi^{-1}(T)$ curves must intercept at the same point ($T=0,y=\Theta_0/C_0$) for all Mn concentrations, as observed in Fig. 2. From this model, and using Eq. (5) we estimated the main (nearest-neighbor) Mn-Mn superexchange integral as $J_1/k_B=8.4(3)$ K. Clearly this value must be taken as approximate, since FM-AFM interactions with second- and higher-nearest neighbors could significantly contribute to J/k_B. It is interesting to note that the $\Theta(x=1)$ value is more than one order of magnitude larger than T_M, i.e., $\Theta/T_M\simeq 25$, with similar ratio values for $x=0.9$ and 0.7 samples. These high Θ/T_M values are consistent with the existence of magnetic frustration expected for a SG system.

B. Dynamic analysis of spin freezing

When approaching the freezing temperature of a spin-glass transition from above, the characteristic relaxation time τ of individual magnetic moments will show a critical slowing down, characterized by a power law $\tau\propto\xi^z$, where ξ is the correlation length and z is called the dynamical scaling exponent. The correlation length ξ itself is related to the reduced temperature $t=(T-T_f)/T_f$, where T_f is the freezing temperature, by the correlation-length critical exponent ν as $\xi\propto t^{-\nu}$. Therefore, the relationship

$$f=f_0\,t^{z\nu} \qquad (6)$$

must be valid near the critical point. Typical values for f_0 are in the 10^{11-12} Hz range for canonical spin glasses, such as

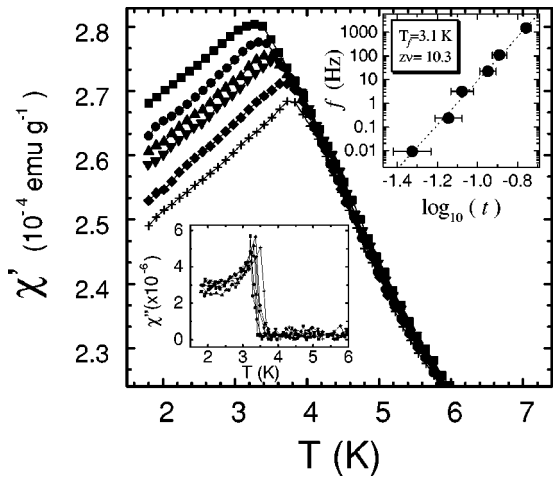

FIG. 3. Main panel: frequency dependence of the in-phase component $\chi(T)$ for $Zn_{0.1}Mn_{0.9}In_2Te_4$ near the freezing temperature T_f. Lower inset: the out-of-phase component $\chi''(T)$. Upper inset: log-log plot of the reduced temperature $t=(T-T_f)/T_f$ vs driven frequency. The solid line is the best fit, using Eq. (6).

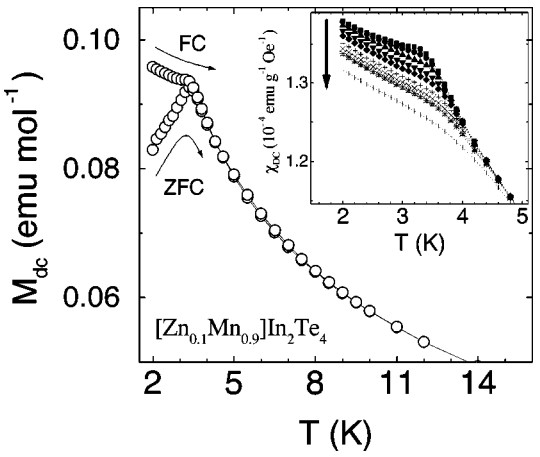

FIG. 4. Zero-field-cooled and field-cooled magnetization curves for the $Zn_{0.1}Mn_{0.9}In_2Te_4$ sample, showing irreversibility for $T<T_M$. Inset: field-cooled $\chi_{dc}(T)=M(T)/H$ curves taken at different fields. The arrow indicates the direction of increasing field from 10 to 2 kOe.

CuMn and AuMn. We have tried to determine whether the maximum observed in the $\chi_{dc}(T)$ curves (for $x\geqslant 0.5$ samples) correspond to a spin-glass transition, by applying the above analysis to the ac susceptibility $\chi_{ac}(T)$ at different frequencies f in a sample with $x=0.9$. The in-phase component $\chi'(T)$, shown in Fig. 3, qualitatively exhibits the behavior expected for spin glasses, i.e., a shift of the cusp to higher temperatures for higher frequencies. However, a more appropriate criterion than the χ' (or χ'') maximum must be chosen to check the validity of Eq. (6), since it defines a set of $T_f(\omega)$ values for which τ is not necessarily constant. Following Bontemps *et al.*,[20] we have used a criterion that involves the quantity

$$\tan\phi=\frac{\chi''}{\chi'}=\omega\tau, \tag{7}$$

setting $\tan\phi\approx\phi=$const, where the constant value was chosen to be small compared to the value at the inflection point. This defines a set of T_f values for which $\omega\tau$ is constant. It is worth noting that the observed scatter in our present $\chi''(T)$ data results in large errors in the estimation of $T_f(\omega)$ values. However, within the narrow temperature range corresponding to ϕ values between 9×10^{-3} deg and 2×10^{-2} deg, it was verified that the resulting T_f values were essentially constant.

The relative variation of T_f per frequency decade $\Delta T_f/[T_f\Delta\log(\omega)]$ is 2.2×10^{-2}, similar to the reported value for *II-IV* DMS systems, in particular for the $Cd_{0.6}Mn_{0.4}Te$ compound.[18] This value lays between those frequency shifts of $\simeq5\times10^{-3}$ observed in CuMn and AuMn canonical spin glasses, and $\simeq6\times10^{-2}$ found in (EuSr)S insulator.[19] When plotted on a log-log graph (see the inset of Fig. 3) the experimental f vs t data showed a linear increase within the available experimental frequency range (six decades), as expected for a spin glass. The best fit using Eq. (6) was obtained for $z\nu=10.3\pm2$, $f_0=1.8\times10^9$ Hz, and $T_f=3.1(2)$ K. The critical exponent value compares quite well with other 3D spin glasses,[21–24] and also with recent studies on 'non-conventional' SG systems like $La_{0.95}Sr_{0.05}CoO_3$ ceramic[25] and interacting Fe-C nanoparticles.[26] We mention here that a complete determination of the critical exponent at the SG transition should be performed by a full dynamic scaling of $\chi''(f,T)$. However, the imaginary part χ'' is about 10^{-2} times smaller than χ' (see the inset of Fig. 3), the former being close to our experimental sensibility. Due to this limitation in our signal-to-noise ratio for the out-of-phase component, the uncertainty in the fit parameters was too high to provide physical insight.

We note also that critical behaviors in disordered systems have been described by many authors using activated dynamics as an alternative to the phase-transition model.[27,28] The activated dynamics model assumes the existence of free-energy barriers for relaxation processes, giving relaxation times that follow a generalized Vogel-Fulcher law $\tau=\tau_0\exp[\varepsilon_0/(T-T_f)^{\varphi\nu}]$, where φ and ν are critical exponents. Applying this law to our data always resulted in poorer fits, giving the (unphysical) results $T_f\approx2.48$ K and $\tau_0\approx10^{-16}$ s.

C. Static analysis of spin freezing

In addition to the frequency dependence of the cusp in $\chi_{ac}(T)$ discussed above, the irreversibility between ZFC and FC modes observed for $x=0.9$ below the maximum of $M(T)$ (see Fig. 4) reinforces the presumption of a spin-glass transition at this temperature. We therefore searched for the expected divergence of the nonlinear static susceptibility at the transition temperature, and examined its critical behavior. The method is based on an analysis of magnetization data measured in field-cooling mode, by expanding $M(H,T)$ in odd powers of H in the $T>T_f$ region,

$$M(T,H)=\chi_0(T)H-\chi_2(T)H^3+\chi_4(T)H^5-\cdots, \tag{8}$$

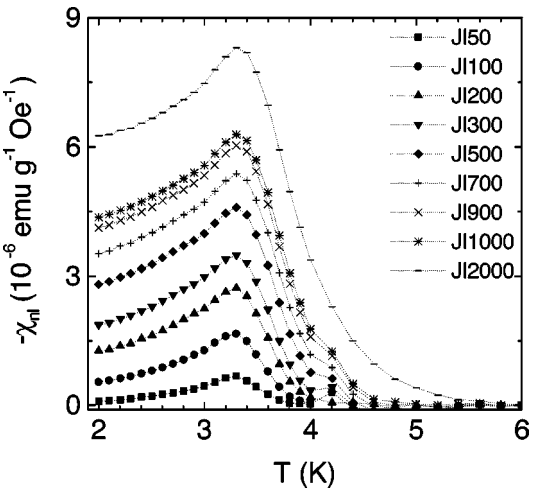

FIG. 5. Nonlinear susceptibility χ_{nl} vs temperature for $Zn_{0.1}Mn_{0.9}In_2Te_4$ at several applied fields. Note the increase of nonlinear terms for $T \rightarrow T_f$.

where $\chi_0(T)$ is the linear susceptibility in the limit $H \rightarrow 0$. The nonlinear susceptibility χ_{nl} is thus defined as

$$\chi_{dc}(T,H) = \chi_0(T) - \chi_2(T)H^2 + \chi_4(T)H^4 - \cdots = \chi_0(T) + \chi_{nl}(T,H) \tag{9}$$

While $\chi \propto T^{-1}$ must be nondivergent at T_f, the nonlinear terms χ_2 and χ_4 should diverge as $(T-T_C)^{-\gamma}$ and $(T-T_C)^{-2(\gamma+\beta)}$, respectively.[29,30] A precise determination of nonlinear coefficients must be restricted to the region near T_f, since regular terms become non-negligible for increasing temperature and applied fields, obscuring the leading χ_2 term. The $\chi_{nl}(T,H)$ components for $x=0.9$ at different fields are plotted in Fig. 5, where the reference field H_0 was taken as the smallest dc field used in this experiment, i.e., 10 Oe. It can be observed that, when approaching T_f from above, the nonlinear component $-\chi_{nl}$ shows the divergentlike behavior expected for a SG transition. In this case, $\chi_{nl}(t,H)$ in the critical region can be related to the critical exponents γ and β by the universal scaling equation[29]

$$\chi_{nl} = t^{\beta}\Phi\left(\frac{H_0^2}{t^{\beta+\gamma}}\right), \tag{10}$$

where $t=(T-T_f)/T_f$ is the reduced temperature. $\Phi(x)$ is a scaling function that satisfies[31]

$$\Phi(x) \rightarrow \begin{cases} x, & \text{for } x \rightarrow 0 \\ \frac{1}{x^{\delta}}, & \text{for } x \rightarrow \infty, \end{cases} \tag{11}$$

where δ is a critical exponent. Small-x values are defined here as the region where the slope of χ_{nl} is linear in H_0^2. The resulting universal curve from experimental data is displayed as a log-log scale plot in Fig. 6 for $T > T_f$. Good scaling of experimental data was achieved with $\beta = 0.9(1)$, $\gamma = 3.6(4)$, and $T_f = 3.4(1)$ K, consistent with the T_f value from ac susceptibility. For temperatures increasingly close to T_f (top right region of the plot), the curve approaches the asymptotic

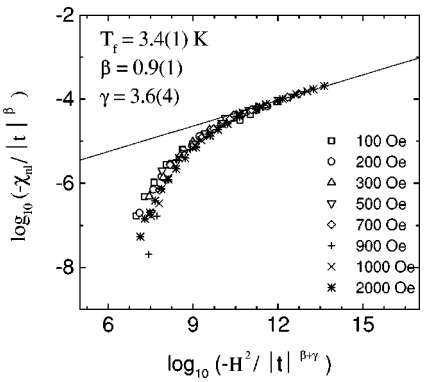

FIG. 6. Nonlinear susceptibility χ_{nl} for $Zn_{0.1}Mn_{0.9}In_2Te_4$ (same data as in Fig. 5) analyzed according to the universal scaling function of Eq. (10). The solid line represents the asymptotic limit of experimental data to the $\beta/(\gamma+\beta)$ value for $T \rightarrow T_f$ (top right part of the graph).

slope $\beta/(\gamma+\beta)$, giving additional support to the conclusion that there is a true spin-glass transition in this compound. It is worth noting that the present data collapse along several orders of magnitude on both axes. In the opposite region of the plot ($T \approx 2T_f$), the superposition shows increasing scatter originated in the vanishing of the nonlinear components of $\chi(T)$ far from the critical region.

IV. DISCUSSION AND CONCLUSIONS

For intermetallic spin glasses, the critical parameters scale with the concentration of magnetic ions, and are therefore unique for a given system at different concentrations. In contrast, insulating spin glasses cannot be scaled in this way, and therefore the critical behavior might change along the concentration line. The existence of single spins, pairs, triplets, or clusters as the concentration of magnetic ions increases, results in different properties, mainly at $T \simeq T_f$ and below. Correspondingly, models based on interacting single spins, interacting clusters or mictomagnetism have been applied depending on concentration. Of course, once the percolation limit is reached (for a given crystal structure) the system can undergo long-range ferromagnetic or antiferromagnetic order with definite T_C or T_N. At the concentration level of $x=0.9$ studied in this work, the appearance of interacting Mn clusters could be expected, since we are working well above both site and bond percolation limits for a 3D crystal. However, no evidence of a cluster-glass transition or an antiferromagnetic transition were found.

Although both static and dynamic experiments are well described in terms of a phase transition at a finite critical temperature, it is worth noting that transition temperatures derived from ac and dc experiments differ by about 10%. As mentioned above, a more appropriate approach to determine dynamic exponents should be done using dynamic scaling of $\chi''(\omega,T)$ through universal functions of the order parameters. But the observed scatter in our present χ'' data is too high to achieve an acceptable collapse of the different plots onto a single curve (e.g., by the criterion that the scattering of the points should not exceed the experimental accuracy).

This limitation should also affect our determination of T_f using conventional power-law analysis, and, therefore, the resulting value should be carefully compared to the static scaling procedure. The critical parameters obtained from static scaling $\beta = 0.9(1)$ and $\gamma = 3.6(4)$ are in agreement with a Heisenberg behavior, which can be understood in terms of the isotropic properties of Mn^{2+} ions. In fact, our values compare well with other insulating and semiconducting like AlMnSi and $CsNiFeF_6$, for which the Heisenberg character is well established.[32,33]

When compared to the isostructural $Cd_{1-x}Mn_xIn_2Te_4$ series of compounds, the obtained β and γ values are in excellent agreement.[34] In particular, the static scaling procedure performed by Campo[35] for $x = 0.85$ yielded $T_f = 3.27$ K, $\beta = 0.9 \pm 0.1$, and $\gamma = 3.6 \pm 0.3$. As discussed in Sec. III C, there is evidence (e.g., the irreversibility of ZFC-FC curves below T_M and dependence of χ_{ac} on frequency) suggesting a spin-glass transition in undiluted $MnIn_2Te_4$, and similar properties have been also reported[36] for $CdIn_2Te_4$, although no scaling analysis has yet been performed on these systems to our knowledge. Morón *et al.*[37] recently reported spin-glass behavior in a $Zn_{1-x}Mn_xGa_2Se_4$ series of compounds, in which Mn^{2+} ions are spatially ordered. But, in contrast to the tellurides, the selenides show a transition from SG behavior to antiferromagnetic ordering somewhere between $x = 0.62$ and 1 ($MnGa_2Se_4$). These facts suggest that randomness in the distribution of Mn ions within the crystal lattice in $Zn_{1-x}Mn_xIn_2Te_4$ may be a key feature of the SG state. Additional evidence of the intrinsic Mn disorder comes from the fact that the present values of critical parameters fall within those reported for the site-disordered DMS spin glasses. For example, reported values of critical exponents in doped II-IV semiconductors like $Cd_{1-x}Mn_xTe$, $Hg_{1-x}Mn_xTe$ and $Zn_{1-x}Mn_xTe$, fall within the $3.3 \leqslant \gamma \leqslant 4.0$ and $0.8 \leqslant \beta \leqslant 1.2$ range.[21,38,39] This similarity also suggests the idea that II-IV and $Zn_{1-x}Mn_xIn_2Te_4$ semiconductors may belong to the same universality class.

ACKNOWLEDGMENTS

We are indebted to Dr. J. Campo for enlightening discussions. This work was supported by the Fundaçao de Amparo à Pesquisa do Estado de São Paulo (FAPESP).

*Email address: goya@macbeth.if.usp.br

[1] R.R.P. Singh, Phys. Rev. Lett. **67**, 899 (1991).
[2] C.L. Henley, Phys. Rev. Lett. **62**, 2056 (1989).
[3] Y.G. Joh, R. Orbach, G.G. Wood, J. Hammann, and E. Vincent, Phys. Rev. Lett. **82**, 438 (1999).
[4] G. Toulouse, Commun. Phys. (London) **2**, 115 (1977); J. Villain, J. Phys. C **10**, 1717 (1977).
[5] H.G. Ballesteros, A. Cruz, L.A. Fernández, V. Martín-Mayor, J. Pech, J.J. Ruiz-Lorenzo, A. Tarancón, P. Téllez, C.L. Ullod, and C. Ungil, Phys. Rev. B **62**, 14 237 (2000).
[6] E. Marinari, V. Martín-Mayor, and A. Pagnani, Phys. Rev. B **62**, 4999 (2000).
[7] K. Binder and A.P. Young, Rev. Mod. Phys. **58**, 801 (1986).
[8] B. Martínez, A. Labarta, R. Rodríguez-Solá, and X. Obradors, Phys. Rev. B **50**, 15 779 (1994).
[9] B. Barbara, A.P. Malozemoff, and Y. Imry, Phys. Rev. Lett. **47**, 1852 (1981).
[10] H. Maletta and W. Felsch, Phys. Rev. B **20**, 1245 (1979).
[11] J.E. Bernard and A. Zunger, Phys. Rev. B **37**, 6835 (1988).
[12] H. Hahn, G. Franck, W. Klinger, A. Meyer, and G. Storger, Z. Anorg. Allg. Chem. **279**, 241 (1955).
[13] G. Delgado, C. Chacón, J.M. Delgado, and V. Sagredo, Phys. Status Solidi A **134**, 61 (1992).
[14] K.G. Nikiforov, in *Progress in Crystal Growth and Characterization of Materials*, edited by J.B. Mullin (Pergamon, Oxford, 1999), Vol. 39, p. 1.
[15] K.J. Range and H.J. Hubner, Z. Naturforsch. B **30**, 145 (1975).
[16] V. Sagredo, P. Silva, M. Díaz, L.M. de Chalbaud, and J. Morales, Phys. Status Solidi B **220**, 237 (2000).
[17] J. Spalek, A. Lewicki, Z. Tarnawski, J.K. Furdyna, R.R. Galazka, and Z. Obuszko, Phys. Rev. B **33**, 3407 (1986).
[18] A. Mauger, J. Ferré, M. Ayadi, and P. Nordblad, Phys. Rev. B **37**, 9022 (1988).
[19] J.A. Mydosh, *Spin Glasses: an Experimental Introduction* (Taylor & Francis, London, 1993), Chap. 3.
[20] N. Bontemps, J. Rajchenbach, R.V. Chamberlin, and R. Orbach, Phys. Rev. B **30**, 6514 (1984).
[21] K. Gunnarsson, P. Svedlindh, P. Nordblad, L. Lundgren, H. Aruga, and A. Ito, Phys. Rev. Lett. **61**, 754 (1988).
[22] B. Leclercq, C. Rigaux, A. Mycielski, and M. Menant, Phys. Rev. B **47**, 6169 (1993).
[23] L. Sandlund, P. Granberg, L. Lundgren, P. Nordblad, P. Svedlindh, J.A. Cowen, and G.G. Kenning, Phys. Rev. B **40**, 869 (1989).
[24] P. Granberg, J. Mattsson, P. Nordblad, L. Lundgren, R. Stubi, J. Bass, D.L. Leslie-Pelecky, and J.A. Cowen, Phys. Rev. B **44**, 4410 (1991).
[25] D.N.H. Nam, R. Mathieu, P. Nordblad, N.V. Khiem, and N.X. Phuc, Phys. Rev. B **62**, 8989 (2000).
[26] P. Jönsson, M.F. Hansen, P. Svendlindh, and P. Nordblad, J. Magn. Magn. Mater. **226-30**, 1315 (2001).
[27] D.S. Fisher and D.A. Huse, Phys. Rev. Lett. **56**, 1601 (1986).
[28] A.P. Malozemoff and E. Pytte, Phys. Rev. B **34**, 6579 (1986).
[29] M. Suzuki, Prog. Theor. Phys. **58**, 1151 (1977).
[30] S. Katsure, Prog. Theor. Phys. **55**, 1049 (1976).
[31] A.B. Surzhenko and V.F. Solovyov, Phys. Rev. B **59**, 11859 (1999).
[32] P. Beauvillain, C. Chappert, J.P. Remard, and J. Seiden, J. Magn. Magn. Mater. **54**, 127 (1986).
[33] C. Pappa, J. Hammann, and C. Jacoboni, J. Phys. (Paris) **46**, 637 (1985).
[34] J. Campo, Ph.D. thesis, University of Zaragoza, 1995.
[35] J. Campo, (unpublished).
[36] F. Palacio, J. Campo, V. Sagredo, L. Betancourt, and J. Morales, Mater. Sci. Forum **182-184**, 459 (1995).
[37] M.C. Morón, J. Campo, F. Palacio, G. Attolini, and C. Pelosi, J. Magn. Magn. Mater. **196**, 437 (1999).

[38] A. Mauger, J. Ferré, and P. Beauvillain, Phys. Rev. B **40**, 862 (1989).

[39] Y. Zhou, C. Rigaux, A. Mycielski, M. Menant, and N. Bontemps, Phys. Rev. B **40**, 8111 (1989); D. Bertrand, A. Mauger, J. Ferré, and P. Beauvillain, *ibid.* **45**, 507 (1992); P.M. Shand, A.D. Christianson, L.S. Martinson, J.W. Schweitzer, T.M. Pekarek, I. Mitokowski, and B.C. Crooker, J. Appl. Phys. B **79**, 6164 (1996).